Meso-α Scale Examination of the 29 March 2000 Dauphin Island, Alabama 'Wedge Tornado's' Pre-Storm Environment

Jeffrey M. Medlin and Matthew Grantham

NOAA-National Weather Service Forecast Office, Mobile, AL

University of South Alabama, Mobile, AL

Introduction and Methodology

During the afternoon of 29 March 2000, a long-lived mesocyclone produced a wedge tornado south of Dauphin Island, Alabama. The tornado and very large-diameter hailstones were captured on video. Using observed upper air, surface and North American Regional Re-Analysis (NARR) data, this study examines a short time period leading up to tornadogenesis. Special focus is given to how the synoptic scale evolution aided the mesocyclone's development. Particular attention is paid to meso-α scale event kinematics, the regional evolution of both thermodynamic instability and vertical wind shear parameters. The observed surface outflow boundary evolution and associated interactions are also examined.

What Happened?

The mesocyclone was initiated over southeastern Louisiana and moved along a surface pressure trough from1832-2134 UTC before approaching the west end of Dauphin Island. A rain-cooled outflow was moving southward but became stationary just north of Dauphin Island as the mesocyclone neared the western end and produce a tornado.

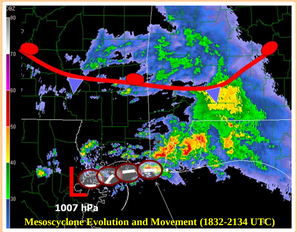

a.

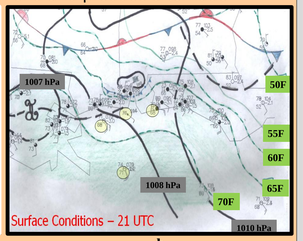

b.

c.

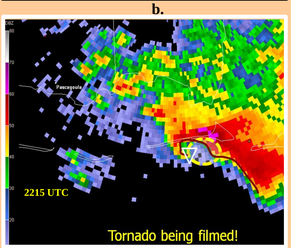

d.

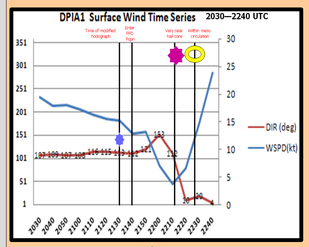

e.

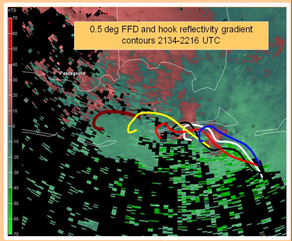

f.

Fig. 1 – Series documenting the **(a)** evolution and movement of the mesocyclone across the Mississippi Sound from 1832-2134 UTC, **(b)** 21 UTC surface conditions, **(c)** existence of a tornado, **(d)** KMOB WSR-88D 0.5° reflectivity product when tornado was occurring (***note** - dashed yellow line is bounded weak echo region drawn to scale), **(e)** Dauphin Island, AL (DPIA1) surface wind time series showing times of modified hodograph (**7a**), forward-flank downdraft precipitation onset, large diameter hail fall and when DPIA1 was within the mesocyclone circulation, and **(f)** 0.5° radar hook and reflectivity gradient streamlines (drawn to scale) from 2134-2216 UTC.

Early Synoptic Evolution

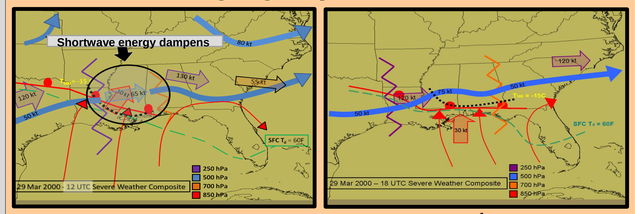

a. b.

Fig. 2 – Synoptic composites taken from mandatory level analyses valid **(a)** 12 UTC and **(b)** 18 UTC (from NARR). Initial shortwave dampened (see **Fig. 2a**). Note re-development of lower tropospheric jet south of the warm front in response to second shortwave arriving from eastern Texas.

21 UTC NARR Upper Air Analyses

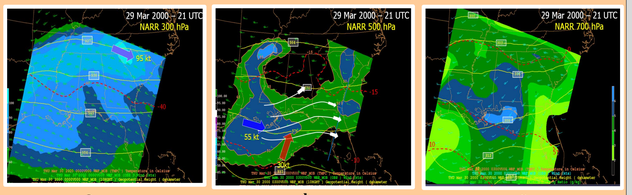

a. b. c.

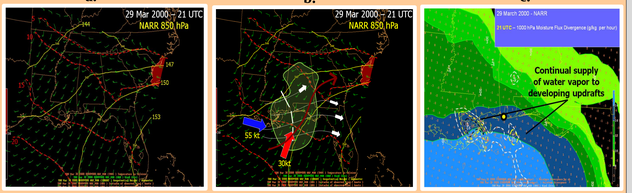

d. e. f.

g. h. i.

Fig. 3 – NARR data for **(a)** 300 hPa **(b)** 500 hPa **(c)** 700 hPa (**d. and e.**) 850 hPa and **(f)** 1000 hPa moisture flux divergence (g kg^{-1} h^{-1}). All fields are labeled in each image. **Figure 3e** shows a compositing of various parameters from **Figs. 3b-d**. **Figures 3g-h** shows surface equivalent potential temperature (K) for 18 and 21 UTC, respectively. **Figure 3i** is a DPIA1 time series of 10m wind speed and 9 m T (C). Surface parcels destabilized very little from 18-21 UTC.

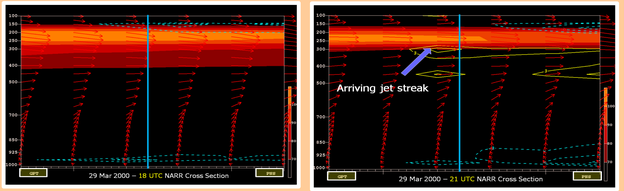

a. b.

Fig. 4 – Sequential NARR Cross-Sections taken from Gulfport, MS (GPT) to Pensacola, FL (PNS) for **(a)** 18 UTC and **(b)** 21 UTC. The blue vertical line represents the approximate longitude of DPIA1. Note the upper level (yellow) and lower level (dashed cyan) divergence (10^{-5} s^{-1}) excited by the arriving jet streak. The synoptic vertical wind profile changes very little.

Vertical Wind Shear and Thermodynamic Instability

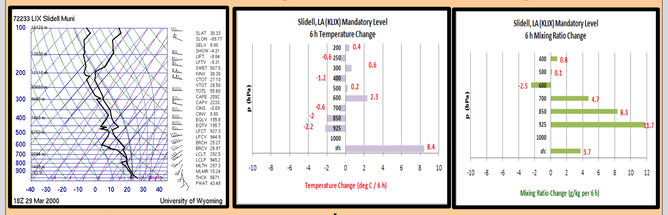

a. b. c.

Fig. 5 – Skew-T log-*p* Profiles for **(a)** Slidell, LA (KLIX), 18 UTC observed and **(b)** KLIX 6 h temperature change (12 to 18 UTC) and **(c)** KLIX 6h mixing ratio change (12 to 18 UTC). The 12 UTC KLIX Skew-T is not shown.

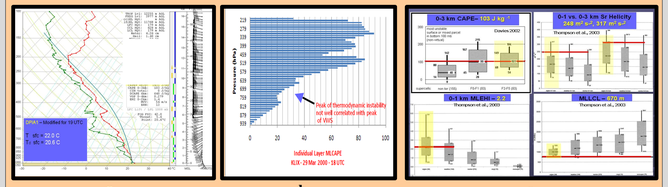

a. b. c.

Fig. 6 – **(a)** DPIA1 Skew-T log-*p* (modified 19 UTC), **(b)** 18 UTC KLIX individual mixed-layer CAPE (MLCAPE, *courtesy David Bright, SPC*) and **(c)** various modified event day thermodynamic and vertical wind shear parameters versus Davies (2003) and Thompson et al., 2003 data sets.

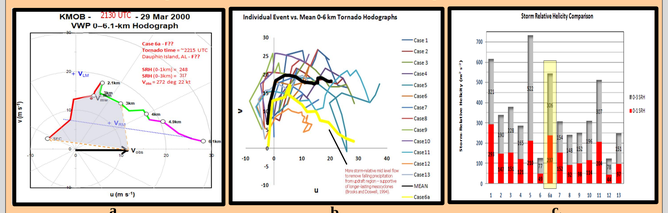

a. b. c.

Fig. 7 – **(a)** KMOB 2130 UTC hodograph **(b)** comparison of case hodograph (yellow – **Case 6a**) to those associated with past regional tornado-producing mesocyclones **(c)** As in **b**. except for 0-1 vs. 0-3 km Sr Helicity (SRH) individual case comparisons . *Hodograph program (***Fig. 7b***) courtesy of Matt Bunkers, NWS Rapid City, SD.*

Outflow Boundary Evolution

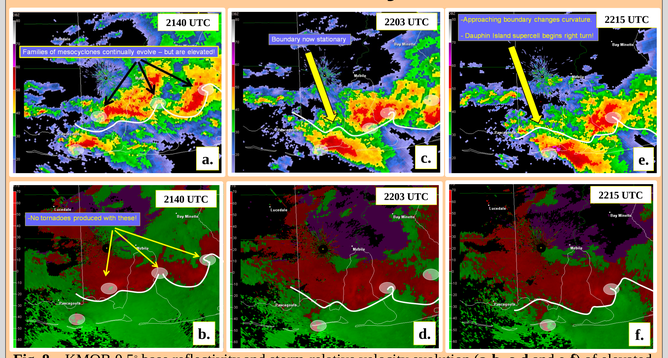

a. c. e.

b. d. f.

Fig. 8 – KMOB 0.5° base reflectivity and storm-relative velocity evolution (**a-b**, **c-d** and **e-f**) of elevated mesocyclones and associated outflow boundaries between 2140-2215 UTC. Note the boundary becomes stationary as the tornado-producing mesocyclone approaches from the west.

Conclusions

• With the early morning lifting out, the event did not initially appear to resemble a 'classic' synoptic severe weather setup. However, closer analysis of NARR data revealed a definite potential for long-lived mesocyclones in the afternoon south of the surface warm front and where vertical wind shear was increasing with time due to the arrival of yet another upper air shortwave. The devil is in the details!

• NARR soundings showed moisture advection significantly moistened the lower and middle troposphere, however, thermal advection did not alter the local vertical thermal profile near the tornado event. The NARR data were supported by thermodynamic changes occurring between 12 and 18 UTC at KLIX (see **Figs 5a-c**).

• Using observed upper air and NARR data to develop a modified sounding near the tornado event, it is pointed out that although SBCAPE was a meager ~1430 J/kg, the 0-3 km CAPE was shown to be ~100 J/kg which lies near the median for ≥F2 intensity tornadoes (Davies 2002). The LCL height of 670 m was near the lowest extrema for *sigtors (* ≥F2 intensity tornadoes) from Thompson et al., 2003. It is believed the vertical distribution of thermodynamic instability was such that low-level updraft accelerations were enhanced in the layer where the greatest vertical wind shear existed (0-1 km).

• The modified proximity hodograph was very similar to 13 other proximity tornado environments near Mobile, AL since 1994. 0-3 km and 0-1 km SRH values were 317 m^2 s^{-2} and 248 m^2 s^{-2} , respectively. Impressively, the 0-1 and 0-3 km SRH event values comparatively lie in the upper quartiles of the Thompson et al., 2003 data set for *sigtors*. It is worth mention that SRH values were enhanced beyond what the ambient vertical wind shear provided due to updraft propagation to the right of the 0-6 km mean wind just prior to tornadogenesis.

• Brooks and Doswell (1994) noted in cases where hodographs are clockwise-curved over the lowest 3 km and linear above, that mesocyclones may be slower to develop but are longer-lived, especially when mid-level shear approaches .010 s^{-1}. Stronger vertical wind shear would suppress the development of a low-level mesocyclone and weaker shear (<.006 s^{-1}) would allow the gust front to undercut the updraft. In this case the 3-6 km mean shear was .009 s^{-1} , consistent with aforementioned findings.

• In this event, elevated mesocyclones that developed north of the outflow boundary shown in **Fig. 8** time series did not produce tornadoes while the mesocyclone to the south did.

• Warning forecasters must be able to detect low-level boundaries in real-time and project their movement. Although a human factors issue, without this awareness, it would have been easy to incorrectly conclude the tornado-producing mesocyclone formed on the southward moving outflow boundary shown in **Figure 8**.

• Of notable interest is how the southward moving outflow boundary not only slowed as it neared the Mobile County Alabama coastline, but it actually became stationary and changed curvature (see **Figs. 8e-f**) as the tornado-producing mesocyclone passed to its south.

• Many environments are supportive of mesocyclones, but most mesocyclones do not produce tornadoes. It is apparent a detailed storm-scale analysis must be undertaken to potentially begin to understand tornadogenesis that occurred in this event. Medlin (2009) performed such an analysis. The analysis revealed the tornado classically formed after the initial BWER and maximum echo top collapse and on the very tip of a radar hook that moved immediately along a very interesting hail swath gradient that developed adjacent to the forward-flank downdraft.

For Further Information

Please Contact: jeff.medlin@noaa.gov